

Shaking Table Test of Irregular Buildings under Horizontal Excitation Acting in an Arbitrary Direction

K.Fujii, T.Ikeda

Chiba Institute of Technology, Japan



ABSTRACT:

In this present article, shaking table tests of multi-story irregular building models are carried out, and the influence of the direction of incidence of seismic input to the response of irregular building is investigated. The results show that the influence of the direction of seismic input to the magnitude of the peak base torque is quite significant; there exists the critical direction of seismic input which produces the largest base torque. The modal decomposition of each test result also reveals that the direction of incidence of which the largest torque occurs is close to the direction that the largest first modal response occurs. Based on these results, it is concluded that the critical direction of each building models is roughly coincide with the principal direction of the first modal response proposed previously by the author.

Keywords: irregular buildings, shaking table test, set-back building

1. INTRODUCTION

In the seismic design of new building structures and also seismic evaluation of existing buildings, the horizontal ground motion is applied along to each main orthogonal axis of the building structures. However it may be insufficient for the irregular buildings because the most critical direction of incidence of seismic input, which would produce the largest response, may different from each main orthogonal axis of building structure. Since the major component of ground motion may act in any directions, it is very important and curious problem which direction is the most severe for given building structure. In this problem, several researchers have investigated the critical direction of seismic input for given building structure by linear and nonlinear time-history analysis (González, 1992, López and Torres, 1997, Sudo, Sera, and Nishikawa, 1996). However there are few investigations in this problem by shaking table test.

In this paper, shaking table tests of multi-story irregular building models are carried, and the influence of the direction of incidence of seismic input to the response of irregular building is investigated. The torsional index based on mode vector also is defined and discussed in this paper.

2. OUTLINE OF SHAKING TABLE TEST

2.1 Building models

The building models considered in this test is two of multi-story irregular building models; three- and two-story irregular building models with setback as shown in Figs. 2.1 and 2.2. All building models are irregular in both plan and elevation; all of them are set-back building model, and the plan of the first floor is L-shaped. The section of column is circular solid and its dimension is 5 mm in diameter. The material used for column is A5052 aluminium. The height of each column is 250mm. The floor slab is consists of two aluminium plate.

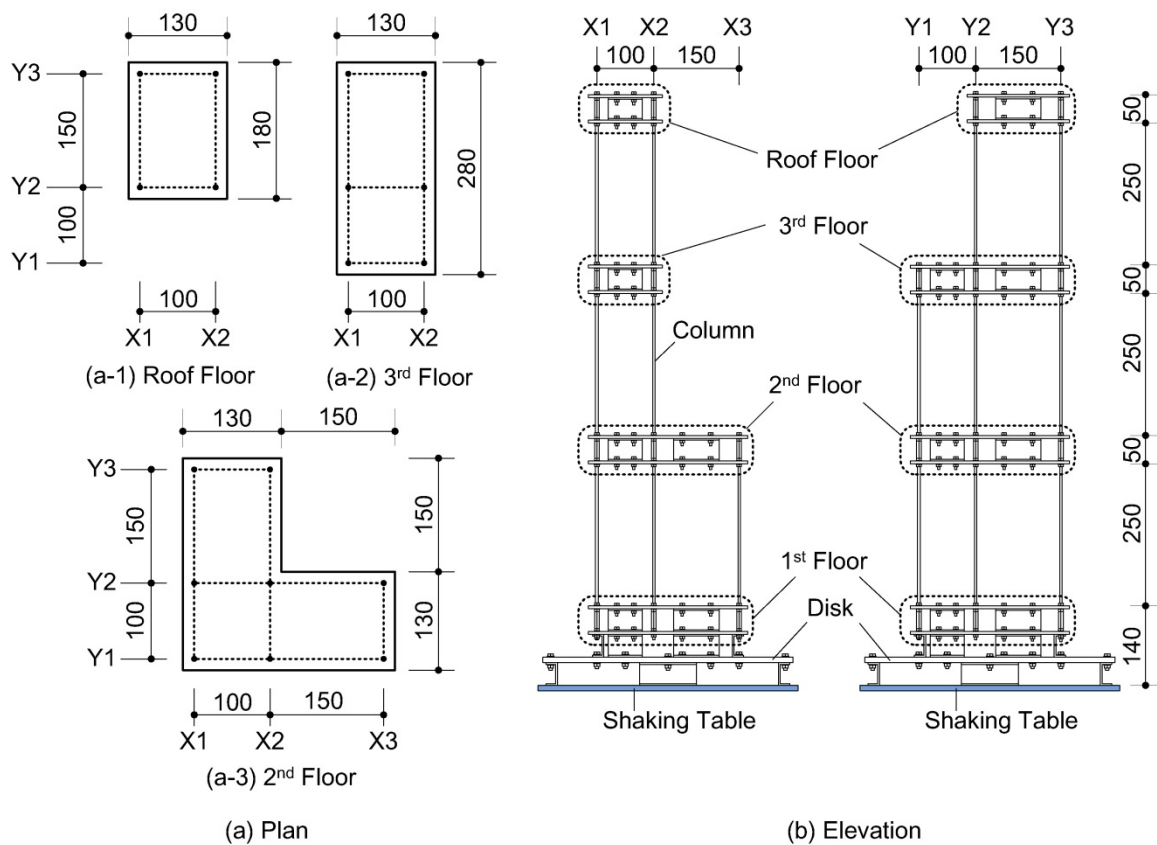


Figure 2.1 Test building model (Three-story building model)

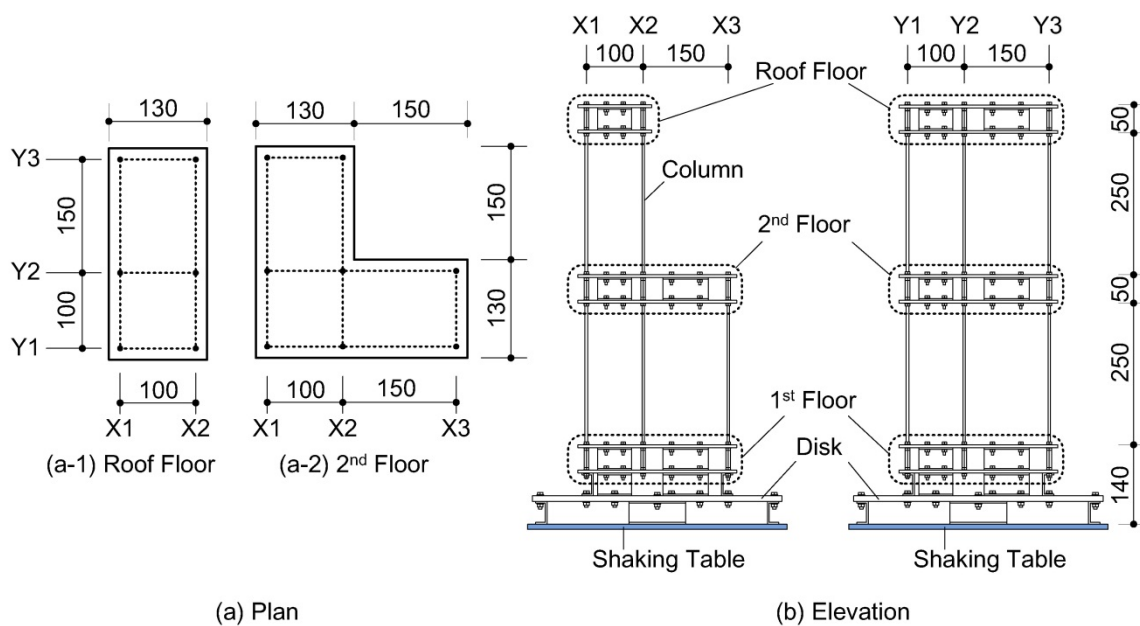


Figure 2.2 Test building model (Two-story building model)

The mass and moment of inertia of each floor obtained from measurement are as follows; for three-story building models (Fig. 2.1), $m_3 = 0.866\text{kg}$ and $I_3 = 3.56 \times 10^{-3} \text{ kgm}^2$ (roof floor), $m_2 = 1.32\text{kg}$ and $I_2 = 1.05 \times 10^{-2} \text{ kgm}^2$ (third floor), and, $m_1 = 1.98\text{kg}$ and $I_1 = 2.39 \times 10^{-2} \text{ kgm}^2$ (second floor), while for two-story building models (Fig. 2.2), $m_2 = 1.32\text{kg}$ and $I_2 = 1.05 \times 10^{-2} \text{ kgm}^2$ (roof floor), and, $m_1 = 1.98\text{kg}$ and $I_1 = 2.39 \times 10^{-2} \text{ kgm}^2$ (second floor), respectively.

Fig. 2.3 shows the natural modes of building models obtained from eigenvalue analysis, assuming that

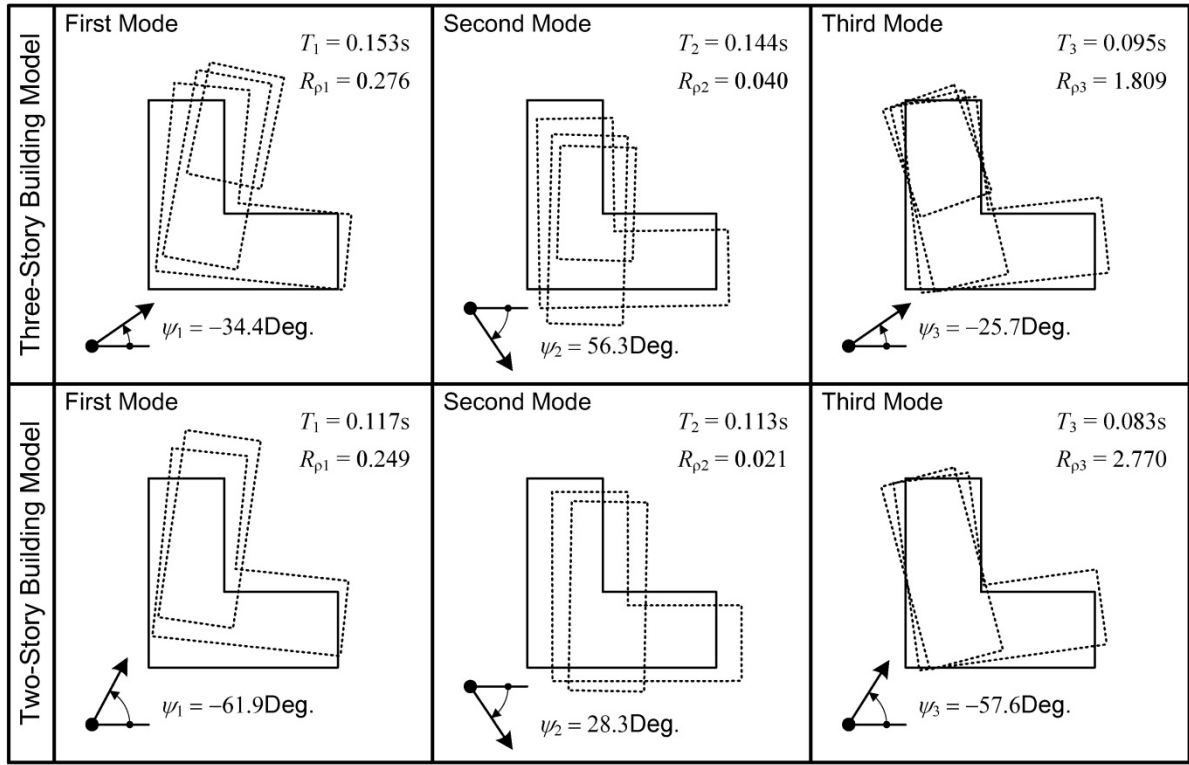


Figure 2.3 Natural modes of building models obtained from analysis

Young's modulus of aluminium rod E is 69GPa. In this figure, T_i is the i -th natural periods, and ψ_i is the angle of incidence of the principal direction of i -th modal response from X-axis, which is defined in previous study by the author (Fujii, 2011) and its tangent is given as Eq.(2.1).

$$\tan \psi_i = - \frac{\sum_j m_j \phi_{yji}}{\sum_j m_j \phi_{xji}} \quad (2.1)$$

In Eq.(2.1), $\phi_i = \{\phi_{x1i} \cdots \phi_{xNi} \quad \phi_{y1i} \cdots \phi_{yNi} \quad \phi_{\theta 1i} \cdots \phi_{\theta Ni}\}^T$ is the i -th natural mode vector. This figure also shows the torsional index of the i -th mode $R_{\rho i}$, defined by Eq.(2.2).

$$R_{\rho i} = \sqrt{\frac{\sum_j I_j \phi_{\theta ji}^2}{\left(\sum_j m_j \phi_{xji}^2 + \sum_j m_j \phi_{yji}^2 \right)}} \quad (2.2)$$

The formulation of the torsional index of the i -th mode, $R_{\rho i}$, is summarized in APPENDIX. This figure shows that the angles between principal directions of the first two modes are close to 90 degree; for three-story building model, $|\psi_2 - \psi_1| = 90.7$ degrees, while for two-story building model, $|\psi_2 - \psi_1| = 90.2$ degrees. This figure also shows that, for both building model, the first mode is predominantly translational ($R_{\rho 1} < 1$) and the second mode is almost purely translational ($R_{\rho 2} \ll 1$), while the third mode is predominantly torsional ($R_{\rho 3} > 1$).

2.2 Excitation system and ground motion

Fig. 2.4 shows the excitation system. In the test, the building model is fixed to a disk which has 24 holes. The direction of excitation is changed by turning the disk to the angle of incidence considered in each test (24 cases for each building model with interval of 15 degrees) as shown in Fig. 2.4 (b), where ψ is the angle of incidence of seismic input from X-axis.

Fig. 2.5 shows the setup of two-story building model. As shown in this figure, the acceleration of all

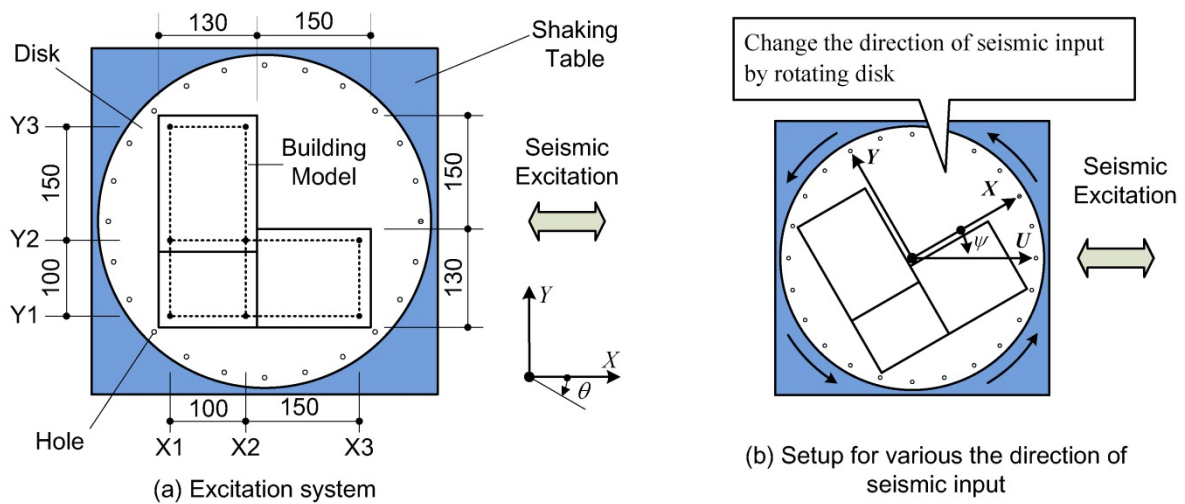


Figure 2.4 Excitation system

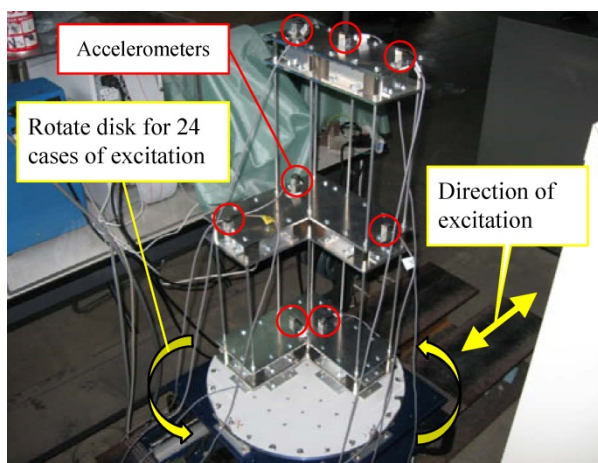


Figure 2.5 Test setup of two-story building model

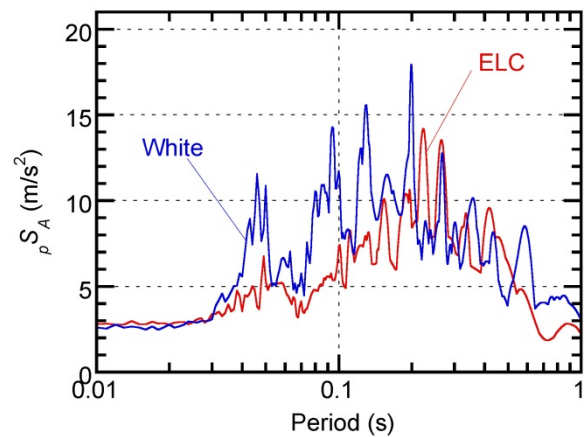


Figure 2.6 Response spectrum of seismic input

floors is measured by accelerometers; on the roof and the second floor, three accelerometers are set to obtain three components of absolute acceleration (X- and Y-direction and rotation) at the center of mass of each floor, while on the first floor two accelerometers are set to measure two components (X- and Y-direction) of accelerations. The sampling interval is 0.001 second.

The time-history of relative displacement at center of mass of each floor is obtained by double-integral of relative acceleration at center of mass of each floor. It should be noted that the double-integral of acceleration is calculated in frequency-domain using Fast Fourier Transform (FFT) and proper filter; the components lower than 2Hz and higher than 15Hz are removed to minimize the influence of numerical noise.

Fig. 2.6 shows the pseudo-acceleration response spectrum of seismic input. Since the damping ratio of building models obtained from white-noise excitation test is 0.01 for the first mode, the response spectrum with damping ratio 0.01 are shown in this figure. As shown in this figure, El Centro 1940 NS ground motion record (ELC) and white noise wave are used to the shaking table test. In this test, the time interval of ELC is scaled half because of the following reasons; i) to simulate the response of middle-rise building with natural period of 0.3 through 0.4 seconds, ii) to adjust the maximum movement of shaking table within the allowable limit, and iii) to adjust the response of building model within elastic range.

3. TEST RESULTS AND DISCUSSION

3.1 Floor acceleration

Fig. 3.1 shows the time-history response of floor absolute acceleration $\mathbf{a}(t)$ (Eq.(3.1)) of three-story building models subjected to ELC excitation.

$$\mathbf{a}(t) = \{a_{x1}(t) \cdots a_{xN}(t) \quad a_{y1}(t) \cdots a_{yN}(t) \quad a_{\theta 1}(t) \cdots a_{\theta N}(t)\}^T \quad (3.1)$$

In this figure, the angle of incidence of seismic input is (a) $\psi = 60$ degree, and (b) $\psi = 150$ degree, respectively. As shown in this figure, the rotational acceleration response $a_{\theta i}(t)$ is more significant in case of (b) $\psi = 150$ degree than (a) $\psi = 60$ degree.

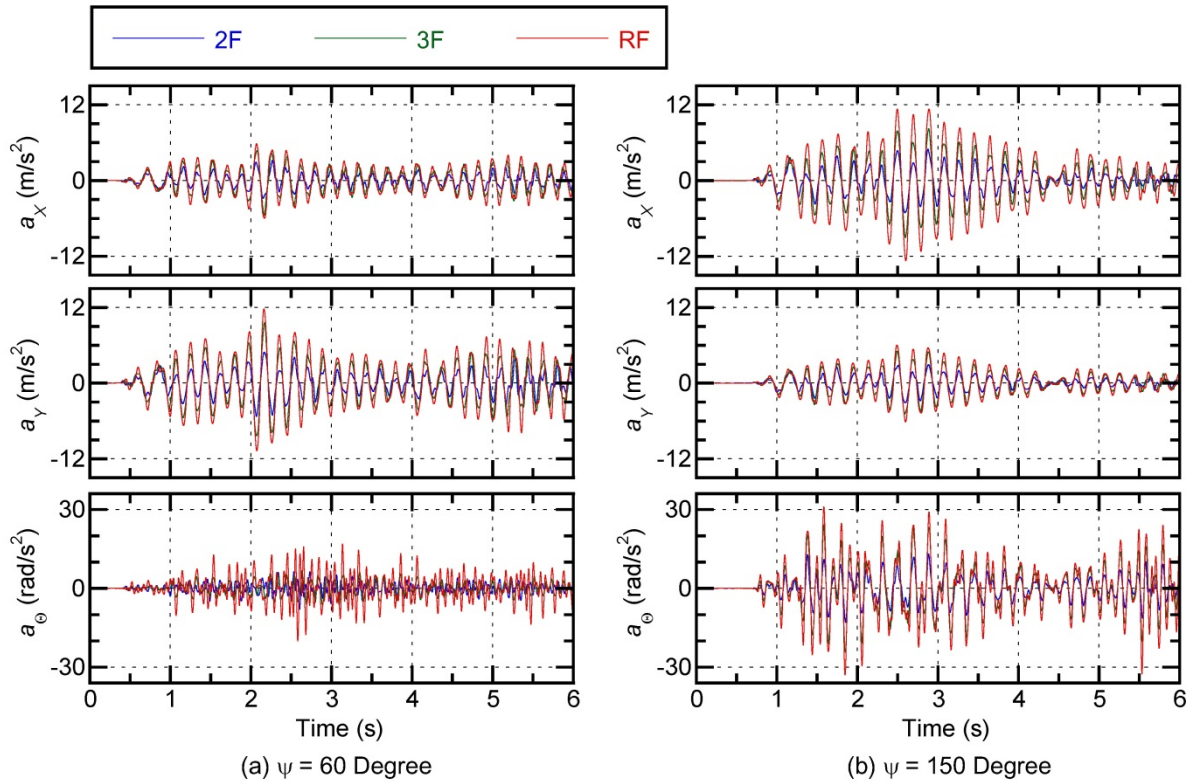


Figure 3.1 Floor acceleration response (Three-story building model, ELC)

3.2 Base shear and torque

Based on the acceleration of all floors, the peak base shear and the peak base torque at center of rigidity is calculated. The X- and Y-component of base shear $V_{X1}(t)$, and $V_{Y1}(t)$ are calculated from Eq.(3.2), and the base torque $T_{Z1}(t)$ is calculated from Eq.(3.3), considering x_{Gj} , y_{Gj} are location of the center of mass of j -th floor and x_{K1} , y_{K1} are location of the center of rigidity of the first story, and hence the peak base shear $V_{1\max}$ and the peak base torsion $T_{Z1\max}$ are obtained from Eq.(3.4).

$$V_{X1}(t) = \sum_j \{-m_j a_{xj}(t)\}, V_{Y1}(t) = -\sum_j \{-m_j a_{yj}(t)\} \quad (3.2)$$

$$T_{Z1}(t) = \sum_j \{-m_j a_{xj}(t)\} (y_{Gj} - y_{K1}) - \sum_j \{-m_j a_{yj}(t)\} (x_{Gj} - x_{K1}) + \sum_j \{-I_j a_{\theta j}(t)\} \quad (3.3)$$

$$V_{1\max} = \left\langle \sqrt{\{V_{X1}(t)\}^2 + \{V_{Y1}(t)\}^2} \right\rangle_{\max}, T_{Z1\max} = |T_{Z1}(t)|_{\max} \quad (3.4)$$

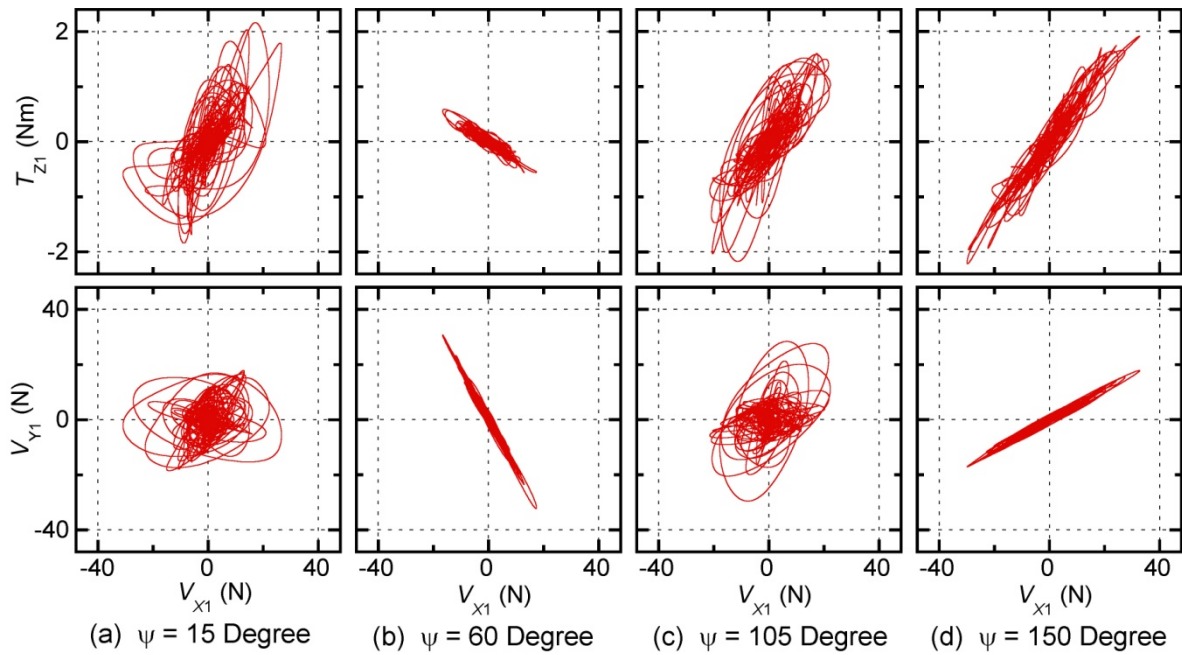


Figure 3.2 Orbit of $T_{Z1}(t) - V_{X1}(t)$ and $V_{Y1}(t) - V_{X1}(t)$ relationship (Three-story building model, ELC)

Fig 3.2 shows the orbit of $T_{Z1}(t) - V_{X1}(t)$ and $V_{Y1}(t) - V_{X1}(t)$ relationship for three-story building model obtained for 4 cases; $\psi = 15, 60, 105,$ and 150 degree. As shown in this figure, the orbit is significantly different in each case. In case of $\psi = 60$ degree, $V_{X1}(t) - V_{Y1}(t)$ orbit shows almost linear behaviour, and $V_{X1}(t) - T_{Z1}(t)$ orbit shows strongly correlated behaviour. Similar observation can be made in case of $\psi = 150$ degree. This implies that single mode response is predominant in these cases. On the contrary, in case of $\psi = 15$ and 105 degree, $T_{Z1}(t) - V_{X1}(t)$ orbit and $V_{Y1}(t) - V_{X1}(t)$ orbit show quite complicated behaviour. This implies that several mode responses are significant in these cases.

Fig. 3.3 shows the relationship of the peak base shear V_{1max} , base torsion T_{Z1max} , to the angle of incidence of seismic input ψ for two building models. As shown in this figure, for both models, the dependent of peak base shear V_{1max} to the direction of seismic input is not significant, while the influence of the direction of seismic input to T_{Z1max} is quite significant. In case of three-story building model, the larger T_{Z1max} is observed in the range of $\psi = 105$ to 150 degree and $\psi = 300$ to 330 degree, while the smaller T_{Z1max} is observed in the range of $\psi = 45$ to 75 degree and $\psi = 225$ to 255 degree. Similar observation can be made of two-story building model.

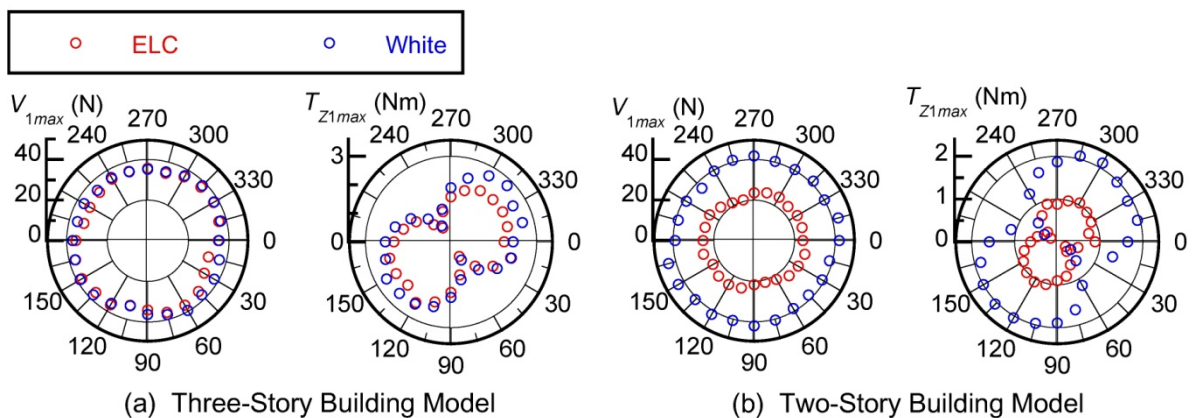


Figure 3.3 Relationship of V_{1max}, T_{Z1max} to the angle of incidence of seismic input ψ

3.3 Modal decomposition

The equivalent acceleration of the i -th modal response with respect to i -th principal direction of modal response, $A_i^*(t)$, is defined by Eq.(3.5).

$$A_i^*(t) = \Gamma_i \boldsymbol{\phi}_i^T \mathbf{M} \mathbf{a}(t) / M_i^* \quad (3.5)$$

$$M_i^* = \Gamma_i^2 \boldsymbol{\phi}_i^T \mathbf{M} \boldsymbol{\phi}_i = \frac{1}{\sum_j m_j \phi_{xji}^2 + \sum_j m_j \phi_{yji}^2 + \sum_j I_j \phi_{\theta ji}^2} \left\{ \left(\sum_j m_j \phi_{xji} \right)^2 + \left(\sum_j m_j \phi_{yji} \right)^2 \right\} \quad (3.6)$$

$$\Gamma_i = \frac{\boldsymbol{\phi}_i^T \mathbf{M} \boldsymbol{\alpha}_i}{\boldsymbol{\phi}_i^T \mathbf{M} \boldsymbol{\phi}_i} = \frac{1}{\sum_j m_j \phi_{xji}^2 + \sum_j m_j \phi_{yji}^2 + \sum_j I_j \phi_{\theta ji}^2} \sqrt{\left(\sum_j m_j \phi_{xji} \right)^2 + \left(\sum_j m_j \phi_{yji} \right)^2} \quad (3.7)$$

$$\mathbf{M} = \begin{bmatrix} \mathbf{M}_0 & \mathbf{0} & \mathbf{0} \\ \mathbf{0} & \mathbf{M}_0 & \mathbf{0} \\ \mathbf{0} & \mathbf{0} & \mathbf{I}_0 \end{bmatrix}, \mathbf{M}_0 = \begin{bmatrix} m_1 & & 0 \\ & \ddots & \\ 0 & & m_N \end{bmatrix}, \mathbf{I}_0 = \begin{bmatrix} I_1 & & 0 \\ & \ddots & \\ 0 & & I_N \end{bmatrix} \quad (3.8)$$

$$\boldsymbol{\alpha}_i = \{\cos \psi_i \cdots \cos \psi_i \quad -\sin \psi_i \cdots -\sin \psi_i \quad 0 \cdots 0\}^T \quad (3.9)$$

In Eq. (3.5), M_i^* and Γ_i are the i -th equivalent modal mass and i -th modal participation factor with respect to i -th principal direction of modal response, respectively. In calculation of $A_i^*(t)$, the mode vectors obtained by eigenvalue analysis (shown in Fig. 2.3) are used, because the response of building model is within the elastic range.

Fig. 3.4 shows the orbit of $A_2^*(t) - A_1^*(t)$ and $A_3^*(t) - A_1^*(t)$ relationship for three-story building model obtained for 4 cases; $\psi = 15, 60, 105,$ and 150 degree. As shown in this figure, $A_1^*(t)$ and $A_3^*(t)$ are negligibly small throughout the response and $A_2^*(t)$ is predominant in case of $\psi = 60$ degree. On the contrary, in case of $\psi = 150$ degree, $A_2^*(t)$ is negligible and $A_1^*(t)$ is predominant. This implies that in case of $\psi = 60$ degree, the second mode response is predominant, while in case of $\psi = 150$ degree, the first mode response is predominant. This figure also shows that, in case of $\psi = 15$ and 105 degree, the response of $A_1^*(t)$, $A_2^*(t)$ and $A_3^*(t)$ are not negligible and their orbits are complicated loops.

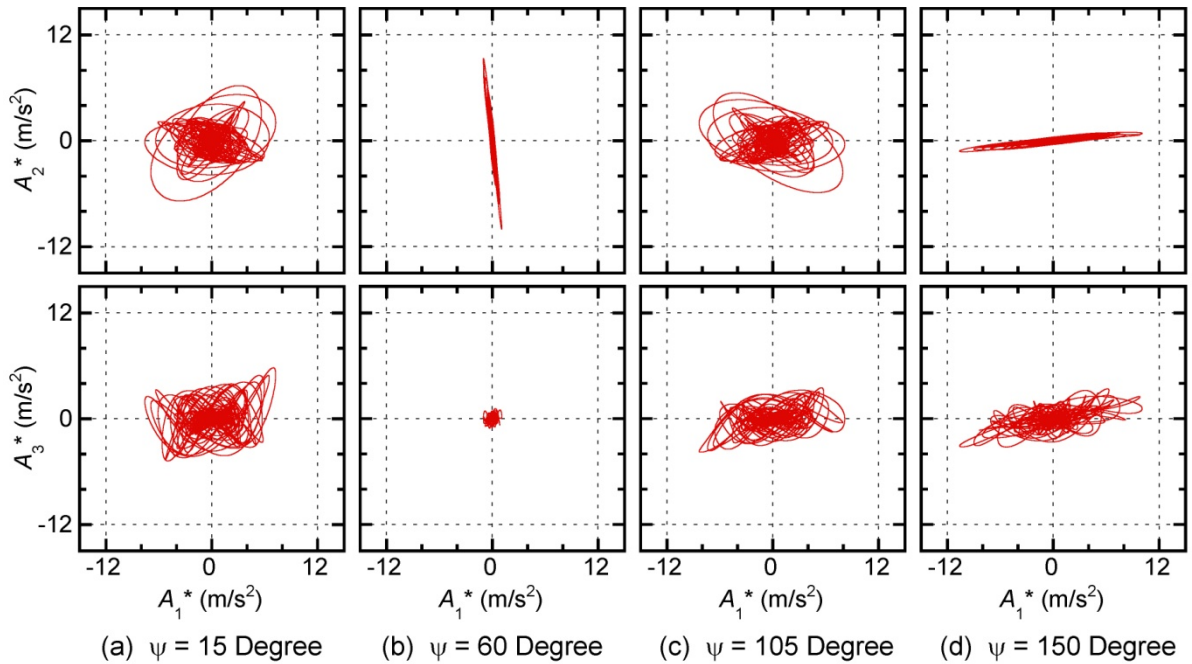


Figure 3.4 Orbit of $A_2^*(t) - A_1^*(t)$ and $A_3^*(t) - A_1^*(t)$ relationship (Three-story building model, ELC)

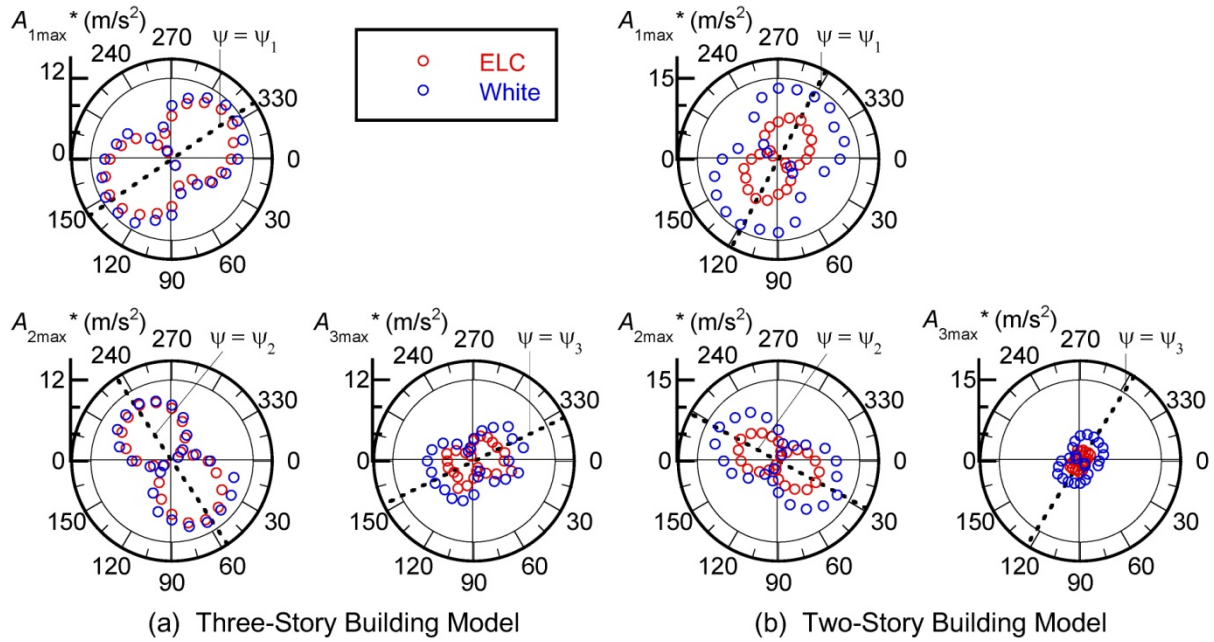


Figure 3.5 Relationship of A_{1max}^* , A_{2max}^* and A_{3max}^* to the angle of incidence of seismic input ψ

Fig. 3.5 shows the relationship of the peak of the i -th modal response with respect to i -th principal direction of modal response, A_{imax}^* and the angle of incidence of seismic input ψ for two building models. In each figure, the principal direction of each modal response is also shown. From this figure, it is evident that the direction in which the largest A_{imax}^* occurs is close to the principal direction of i -th modal response, while the direction in which the smallest A_{imax}^* occurs is perpendicular to the principal direction of i -th modal response.

It is very interesting and important to point out that, to make comparisons with Figs. 3.3 and 3.5, the direction of incidence of which the largest T_{Z1max} occurs is close to the direction that the largest first modal response occurs, while the direction of incidence of which the smallest T_{Z1max} is close to the direction that the largest second modal response occurs. This can be interpreted as follows; as shown in Fig. 2.3, the first and third modes are combination of translational and torsional modes, while the second mode is almost purely translational mode. So in case of the direction of seismic input is close to the principal direction of the second modal response, the building model oscillates predominantly by the second mode and the contribution of the first and third mode is negligibly small, and therefore the torsional response is the smallest. On the contrary, in case of the direction of seismic input is close to the principal direction of the first modal response, the building model oscillates predominantly by the first mode and the contribution of the second mode is negligibly small.

3.4 Peak drift of column

Fig 3.6 shows the relationship of the peak drift of columns in the first story (column X1-Y1, X1-Y3, and X3-Y1) and the angle of incidence of seismic input ψ for two building models. In this figure, the drift of each column is calculated from the time-history of relative displacement at center of mass of each floor. As shown in this figure, the most critical column of both model buildings is column X1-Y3, and its largest peak drift occurs in case of ψ is close to ψ_1 . It should be also pointed out that the largest peak drift of column X3-Y1 occurs in case of ψ is close to ψ_2 , while its smallest peak drift occurs in case of ψ is close to ψ_1 . This can be easily explained from the first mode shape shown in Fig. 2.3; in case of the building models oscillate in the first mode, the largest drift occurs at column X1-Y3 while the smallest occurs at column X3-Y1.

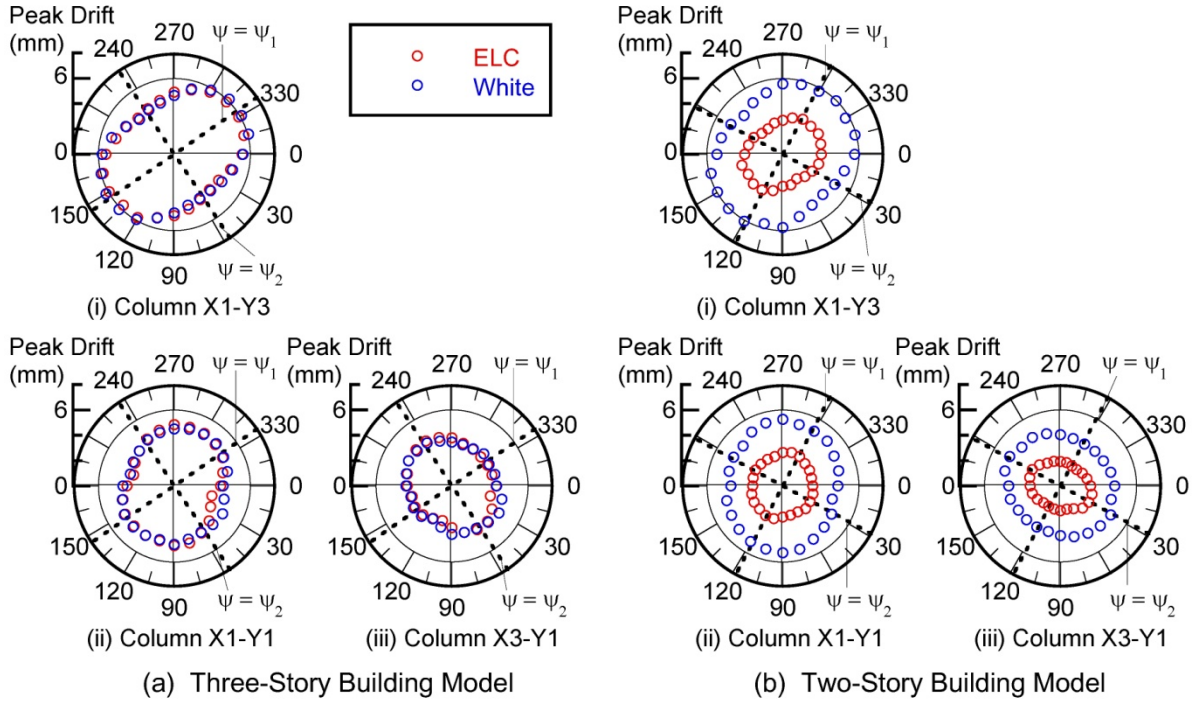


Figure 3.6 Relationship of peak drift of columns to the angle of incidence of seismic input ψ

4. CONCLUSIONS

In this present article, shaking table tests of multi-story irregular building models with set-back are carried, and the influence of the direction of incidence of seismic input to the response of irregular building is investigated. Based on these results, it is concluded that the critical direction of each building models is roughly coincide with the principal direction of the first modal response.

APPENDIX. FORMULATION OF TORSIONAL INDEX BASED ON MODE SHAPE

The i -th equivalent modal mass with respect to i -th principal direction of modal response M_i^* is expressed as Eq. (A1), which is identical with Eq. (3.6). Assuming that from Eq. (A1) the i -th mode is purely translational ($\phi_{\Theta ji} = 0$), the i -th equivalent modal mass neglecting the rotational component M_{iT}^* can be expressed as Eq. (A2).

$$M_i^* = \frac{1}{\sum_j m_j \phi_{Xji}^2 + \sum_j m_j \phi_{Yji}^2 + \sum_j I_j \phi_{\Theta ji}^2} \left\{ \left(\sum_j m_j \phi_{Xji} \right)^2 + \left(\sum_j m_j \phi_{Yji} \right)^2 \right\} \quad (\text{A1})$$

$$M_{iT}^* = \frac{1}{\sum_j m_j \phi_{Xji}^2 + \sum_j m_j \phi_{Yji}^2} \left\{ \left(\sum_j m_j \phi_{Xji} \right)^2 + \left(\sum_j m_j \phi_{Yji} \right)^2 \right\} \quad (\text{A2})$$

From Eqs. (A1) and (A2), the ratio (M_{iT}^* / M_i^*) is obtained as shown in Eq. (A3).

$$\frac{M_{iT}^*}{M_i^*} = \frac{1}{\sum_j m_j \phi_{Xji}^2 + \sum_j m_j \phi_{Yji}^2 + \sum_j I_j \phi_{\Theta ji}^2} \left(\sum_j m_j \phi_{Xji}^2 + \sum_j m_j \phi_{Yji}^2 \right) \quad (\text{A3})$$

In Eq. (A3), the ratio (M_{iT}^* / M_i^*) is the reduction ratio of i -th equivalent modal mass due to rotational component; if i -th mode is purely translational mode, (M_{iT}^* / M_i^*) is unity, while if it is purely torsional mode, (M_{iT}^* / M_i^*) is zero. Eq. (A3) can be rewritten as Eq. (A4), considering the torsional index of the i -th mode, $R_{\rho i}$, defined by Eq. (A5), which is identical with Eq.(2.2).

$$\frac{M_{iT}^*}{M_i^*} = \frac{1}{1 + R_{\rho i}^2} \quad (A4)$$

$$R_{\rho i} = \sqrt{\frac{\sum_j I_j \phi_{\Theta j i}^2}{\left(\sum_j m_j \phi_{x j i}^2 + \sum_j m_j \phi_{y j i}^2 \right)}} \quad (A5)$$

From Eq. (A4), it can be seen that the ratio (M_{iT}^* / M_i^*) is unity in case of $R_{\rho i}$ is zero (purely translational), while (M_{iT}^* / M_i^*) is close to zero in case of $R_{\rho i}$ is significantly large. Therefore, the term “predominantly translational” and “predominantly torsional” can be defined by using $R_{\rho i}$; “predominantly translational” mode is the mode in case of $R_{\rho i} < 1$, while “predominantly torsional” mode is the mode in case of $R_{\rho i} > 1$. It should be pointed out that the index $R_{\rho i}$ can be used for both single-story and multi-story irregular buildings.

AKNOWLEDGEMENT

The author acknowledges support by Grant-in-Aid for Young Scientist (Category (B), No. 21760443), Japan Ministry of Education, Culture, Sport, Science and Technology (MEXT).

REFERENCES

- González, P. (1992). Considering earthquake direction on seismic analysis. *Proceedings of the Tenth World Conference on Earthquake Engineering*. **7**: 3809-3913.
- López, O. A., Torres, R. (1997). The critical angle of seismic incidence and the maximum structural response. *Earthquake Engineering and Structural Dynamics*. **26**, 881-894.
- Sudo, S., Sera, K. and Nishikawa, T. (1996). Torsional response analysis of buildings subjected to bi-directional ground motions. *Proceedings of the Eleventh World Conference on Earthquake Engineering*. Paper No. 865.
- Fujii, K. (2011). Nonlinear static procedure for multi-story asymmetric frame buildings considering bi-directional excitation. *Journal of Earthquake Engineering*. **15**, 245-273.